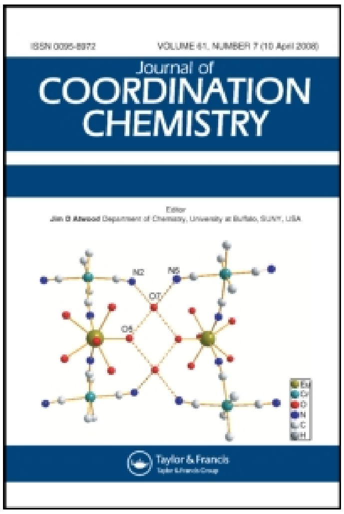

Journal of Coordination Chemistry
Publication details, including instructions for authors and subscription information:
http://www.informaworld.com/smpp/title~content=t713455674

Inclusion cages constructed from trinuclear linear Zn^{II}/Co^{II} building blocks

Shu Sun[a]; Sanping Chen[a]; Shengli Gao[a]
[a] Department of Chemistry, Shaanxi Key Laboratory of Physico-Inorganic Chemistry, Northwest University, Xi'an, Shaanxi 710069, P.R. China

To cite this Article Sun, Shu , Chen, Sanping and Gao, Shengli(2008) 'Inclusion cages constructed from trinuclear linear Zn^{II}/Co^{II} building blocks', Journal of Coordination Chemistry, 61: 13, 2068 — 2078
To link to this Article: DOI: 10.1080/00958970701866135
URL: http://dx.doi.org/10.1080/00958970701866135

Journal of Coordination Chemistry
Vol. 61, No. 13, 10 July 2008, 2068–2078

Inclusion cages constructed from trinuclear linear Zn^{II}/Co^{II} building blocks

SHU SUN, SANPING CHEN and SHENGLI GAO*

Department of Chemistry, Shaanxi Key Laboratory of Physico-Inorganic Chemistry,
Northwest University, Xi'an, Shaanxi 710069, P.R. China

(*Received 4 April 2007; in final form 13 August 2007*)

Two 3D isostructures of $\{[M_5(atrz)_6(\mu_2\text{-}O)](NO_3)_2(H_2O)_6\}_\infty$ ($\mathbf{1}\cdot M(NO_3)_2(H_2O)_6$; $M = Zn^{II}$, Co^{II}; atrz = 3-amino-1H-1,2,4-triazole anion) have been obtained *via* hydrothermal techniques. Both crystallize in the cubic space group $Pa\bar{3}$ with $a = 15.0416(2)$ Å, $V = 3403.16(8)$ Å^3, $Z = 4$ for $\mathbf{1}\cdot Zn$ and $a = 15.046(2)$ Å, $V = 3406.1(9)$ Å^3, $Z = 4$ for $\mathbf{1}\cdot Co$. The framework of **1** consists of $[M_3(atrz)_6]$ ($M = Zn^{II}$, Co^{II}), trinuclear linear M^{II} building block, linked through tetrahedral sites of $[MN_3O]$, extending to a 3D structure containing numerous cages in which $2n$ NO^{3-} and $6n$ H_2O are locked. In **1**, M^{II} ions show octahedral and tetrahedral coordination geometries and atrz are three-connected nodes. The polymers were characterized by single-crystal X-ray diffraction, thermogravimetric analysis (TGA), elemental analysis and infrared spectroscopy.

Keywords: Trinuclear linear; Zn^{II}; Co^{II}; 1,2,4-Triazole; Crystal structure

1. Introduction

Metal-organic coordination polymers have potential applications to catalysis, gas storage, separation, and sensing [1–9]. The diversity of properties associated with these materials reflects a vast compositional range which allows variations in covalency, geometry, oxidation states, and crystalline architecture, providing different pore structures, coordination sites, or juxtapositions of functional groups [9–13]. In the specific case of pore structures, the frameworks must be architecturally robust so that upon removal of the guest molecules, the pore structure is maintained and the interior volume is fully accessible to sorbate molecules. To date, a large number of coordination polymers based on polynuclear metal clusters have been explored [14–16], however, most of the organic ligands are multitopic carboxylate and pyridine as linkers [17–21]; alternative tether lengths, charge-balance requirements, or orientations of donor groups may afford advantages in the design of materials.

Polyaza heterocycle Htrz (1,2,4-triazole) and its derivatives are ligands, which have such properties. As one of the simplest 1,2,4-triazole derivatives, Hatrz (3-amino-1H-1,2,4-triazole) bears the following virtues: (i) diverse bridging modes ($\mu_{1,2}$, $\mu_{2,4}$, and $\mu_{1,2,4}$) to afford polynuclear complexes and polynuclear metal-organic

---

*Corresponding author. Email: gaoshli@nwu.edu.cn

Journal of Coordination Chemistry
ISSN 0095-8972 print/ISSN 1029-0389 online © 2008 Taylor & Francis
DOI: 10.1080/00958970701866135

substructures [22, 23]. (ii) The superexchange capacity and spin crossover with Fe(II), which are reflected in the unusual magnetic properties of triazole complexes [24–27]. The characteristic of Hatrz is the amino group, a potential N-ligating donor, and determines the molecule as an achiral asymmetrically substituted ligand. Li *et al.* obtained a chiral cadmium coordination polymer, $[Cd(atrz)Cl]_\infty$, based on the achiral unsymmetrical atrz anion with an unprecedented μ_4-bridging mode [28].

Though trinuclear linear M^{II} subunits defined by triple triazole bridges are often encountered in polynuclear complexes of triazoles [22, 29–33], no extended framework based on trinuclear linear Zn^{II}/Co^{II} building blocks has been reported [27, 34] and it remains a challenge to prepare new trinuclear linear Zn^{II}/Co^{II}-based solid materials with 3D architectures. Herein we report two isostructural compounds, $\mathbf{1} \cdot M[(NO_3)_2(H_2O)_6]_\infty$ $(M = Zn, Co)$, which are the first 3D organic-inorganic architectures constructed from trinuclear linear Zn^{II}/Co^{II} subunits as building blocks by coordination interactions. The framework of **1** contains numerous cages occupied by the $[(NO_3)_2(H_2O)_6]_\infty$ *via* noncoordinative interactions. The occupancy volumes of both the nitrate anions and solvent molecules are 926.3 $Å^3$ ($\mathbf{1} \cdot Zn$) and 952.7 $Å^3$ ($\mathbf{1} \cdot Co$), accounting for 27.2% and 28.0% of the total cell volumes.

2. Experimental

2.1. *Reagents and instruments*

Commercially available reagents were used as received without further purification. Elemental analyses of C, H, and N were performed on a Vario EL analyzer. Infrared spectra were obtained from KBr pellets on a BEQ VZNDX 550 FTIR instrument within 400–4000 cm^{-1}. ICP-AES experiments were carried out on a T. E. IRIS advantage inductively coupled plasma atomic emission spectrophotometer. Thermogravimetric analysis was carried out on a TA Instruments NETZSCH STA 449C simultaneous TGA–DSC with a heating rate of 10°C min^{-1} under hydrostatic air.

2.2. *Preparation*

$\mathbf{1} \cdot Zn(NO_3)_2(H_2O)_6$. Method A: a mixture of $Zn(NO_3)_2 \cdot 6H_2O$ (0.119 g, 0.40 mmol), Hatrz (0.034 g, 0.40 mmol), py (0.032 g, 0.40 mmol), $HClO_4$ (0.020 g, 0.20 mmol) and H_2O (6 g, 333 mmol) was stirred briefly before sealing in an 8-mL Teflon-lined reactor, then heated at 160°C for 72 h and slowly cooled to 100°C at 5°C per hour. Colorless and/or pale-yellow octahedral crystals were isolated in 19% yield (based on Zn). IR (KBr pellet): ν 3627(m), 3451(s), 2961(w), 2509(w), 1741(w), 1621(s), 1550(s), 1518(s), 1381(s), 1289(m), 1223(m), 1050(m), 941(w), 873(w), 753(w), 624(m) cm^{-1}. Elemental analysis (%) Calcd for $C_{12}H_{30}N_{26}Zn_5O_{13}$: H, 2.82; C, 13.43; N, 33.92; Zn, 30.46. Found: H, 2.68; C, 13.41; N, 34.17; Zn, 30.13.

Caution! *Although no problems were encountered in this study, transition-metal perchlorate complexes are potentially explosive, and furthermore, perchloric acid should be handled with proper precautions for its strong oxidation.*

Method B: a mixture of $Zn(NO_3)_2 \cdot 6H_2O$ (0.119 g, 0.40 mmol), H_2atc (3-amino-1H-1,2,4-triazole-5-carboxylic acid) (0.069 g, 0.50 mmol), NaOH (0.010 g, 0.25 mmol) and

H_2O (6 g, 333 mmol) was stirred briefly before sealing in an 8-mL Teflon-lined reactor, then heated at 170°C for 72 h and slowly cooled to 100°C by 5°C per hour. Colorless and/or pale-yellow crystals, suitable for X-ray diffraction were collected in 21% yield (based on Zn). IR (KBr pellet): ν 3628(m), 3451(s), 2962(w), 2508(w), 1741(w), 1621(s), 1550(s), 1518(s), 1381(s), 1290(m), 1223(m), 1050(m), 941(w), 873(w), 753(w), 624(m) cm^{-1}. Elemental analysis (%) Calcd for $C_{12}H_{30}N_{26}Zn_5O_{13}$: H, 2.82; C, 13.43; N, 33.92; Zn, 30.46. Found: H, 2.71; C, 13.40; N, 34.11; Zn 30.20.

1 · $Co(NO_3)_2(H_2O)_6$. Method A: a mixture of $Co(NO_3)_2 \cdot 6H_2O$ (0.087 g, 0.30 mmol), $Zn(NO_3)_2 \cdot 6H_2O$ (0.089 g, 0.30 mmol), Hatrz (0.034 g, 0.40 mmol), $NH_3 \cdot H_2O$ (0.03 ml, 25%~28%) and H_2O (6 g, 333 mmol) was stirred briefly before sealing in an 8-mL Teflon-lined stainless steel reactor, then heated at 145°C for 72 h and slowly cooled to 100°C at 5°C per hour. Mauve crystals were isolated in 32% yield (based on Co). IR (KBr pellet): ν 3625(m), 3450(s), 2964(w), 2505(w), 1740(w), 1623(s), 1550(s), 1520(s), 1380(s), 1290(m), 1223(m), 1052(m), 940(w), 870(w), 755(w), 622(m) cm^{-1}. Elemental analysis (%) Calcd for $C_{12}H_{30}N_{26}Co_5O_{13}$: H, 2.90; C, 13.84; N, 34.98; Co, 28.30. Found: H, 2.83; C, 13.86; N, 35.07; Co, 28.01.

Method B: the reaction was carried out with a similar method using H_2atc instead of Hatrz. Mauve crystals, suitable for X-ray diffraction, were collected in 13% yield (based on Co). IR (KBr pellet): ν 3625(m), 3450(s), 2963(w), 2505(w), 1740(w), 1623(s), 1550(s), 1520(s), 1380(s), 1290(m), 1223(m), 1052(m), 940(w), 870(w), 755(w), 622(m) cm^{-1}. Elemental analysis (%) Calcd for $C_{12}H_{30}N_{26}Co_5O_{13}$: H, 2.90; C, 13.84; N, 34.98; Co, 28.30. Found: H, 2.76; C, 13.81; N, 35.05; Co, 28.15.

2.3. *X-ray crystallography*

Diffraction intensities of **1** were collected on a Bruker SMART diffractometer with graphite monochromated Mo Kα radiation ($\lambda = 0.71073$ Å) at 273 K. Absorption corrections were applied by using SADABS [35]. The structure was solved by direct methods and successive Fourier difference syntheses (SHELXS-97); anisotropic thermal parameters for all nonhydrogen atoms were refined by full-matrix least-squares procedure against F^2 (SHELXL-97) [36, 37]. Hydrogen atoms were located by geometric calculations. Crystal data and details on refinements are summarized in table 1. Selected bond distances and angles are listed in table 2. The CCDC contains the supplementary crystallographic data for this article, which can be obtained free of charge from The Cambridge Crystallographic Data Center *via* www.ccdc.cam.ac.uk/data_request/cif

3. Results and discussion

3.1. *Preparations*

In Method A, the target products **1** · M (M = Co, Zn) are obtained using Hatrz, but suitable crystals for X-ray diffraction were not obtained. To obtain suitable crystals for X-ray diffraction, H_2atc (3-amino-1H-1,2,4-triazole-5-carboxylic acid) is employed based on the fact that it could be readily decarboxylated to form Hatrz under hydrothermal conditions [38], simultaneously, a spontaneous deprotonation of Hatrz

Table 1. Crystal data and structure refinement information for **1 · Zn/Co**.

Compound	**1·Zn**	**1·Co**
Formula	$C_{12}H_{30}Zn_5N_{26}O_{13}$	$C_{12}H_{30}Co_5N_{26}O_{13}$
Fw	1073.47	1041.20
Crystal system	Cubic	Cubic
Space group	$Pa\bar{3}$	$Pa\bar{3}$
$a=b=c$ (Å)	15.0416(2)	15.046(2)
$\alpha=\beta=\gamma$ (°)	90	90
V (Å^3)	3403.16(8)	3406.1(9)
Z	4	4
F(000)	2216	1888
ρ (Mg m^{-3})	2.158	2.093
Absolute coefficient (mm^{-1})	3.579	2.461
Data/restraints/parameters	1302/0/99	985/12/93
GOF	1.086	1.035
R_1[a] $[I=2\sigma(I)]$	0.0363	0.0442
wR_2[a] (all data)	0.1075	0.1209

[a] $R_1 = \sum ||F_o| - |F_c|| / \sum |F_o|$; $wR_2 = [\sum w(F_o^2 - F_c^2)^2 / \sum w(F_o^2)^2]^{1/2}$.

Table 2. Bond Lengths (Å) and Angles (deg) for **1·Zn/Co**.[a]

	1·Zn	**1·Co**
M(1)–O#1	1.880(8)	1.848(13)
M(3)–O	1.920(8)	1.930(13)
M(1)–N(1)	2.004(3)	2.006(4)
M(2)–N(2)	2.201(3)	2.196(4)
M(3)–N(4)	2.002(3)	2.002(4)
O#1–M(1)–N(1)#4	110.1(6)	109.4(9)
O#1–M(1)–N(1)#5	103.4(6)	105.1(7)
O#1–M(1)–N(1)	137.5(3)	138.3(5)
O–M(3)–N(4)#6	127.7(5)	128.1(6)
O–M(3)–N(4)#7	110.2(7)	108.9(9)
O–M(3)–N(4)	93.7(4)	94.9(6)
N(2)#8–M(2)–N(2)	88.27(10)	88.26(15)
N(2)#8–M(2)–N(2)#5	180.00(12)	180.000(1)
N(1)#4–M(1)–N(1)#5	99.99(11)	99.23(16)
N(4)–M(3)–N(4)#6	107.68(10)	107.63(15)
M(1)#13–O–M(3)	139.9(5)	140.7(7)

[a] Symmetry transformations used to generate equivalent atoms: #1, x, $-y+1/2$, $z+1/2$; #4, y, $z-1$, $x+1$; #5, $z-1$, x, $y+1$; #6, $-y+1/2$, $-z+1$, $x+1/2$; #7, $z-1/2$, $-x+1/2$, $-y+1$; #8, $-z+1$, $-x$, $-y+1$; #9, $-y$, $-z+1$,$-x+1$; #10 $-x$, $-y$, $-z+2$; #11, $-z+3/2$,$-x+1$, $y+1/2$; #12, $-y+1$, $z-1/2$, $-x+3/2$; #13, x, $-y+1/2$, $z-1/2$.

occurs [39]. Decarboxylation was also observed for the related ligand 1,2,4-triazole-3-carboxylic acid under similar reaction conditions [41]. Complexes of the same composition were obtained in Method A and B, while suitable crystals are obtained from Method B. After hydrothermal reaction the solutions of all are pH ~5. It was unanticipated that complexes of **1** · M (M = Co, Zn) are insoluble in all solvents tried (e.g. CH_3COCH_3, CH_3CN, $CHCl_3$, DMF, and DMSO). So, once obtained the complexes cannot be recrystallized.

We cannot obtain **1** · $Co(NO_3)_2(H_2O)_6$ in the similar experimental conditions as **1** · $Zn(NO_3)_2(H_2O)_6$, except as dusty mauve unidentified impurity. Considering the radius of Co^{2+} is identical with that of Zn^{2+}, we supposed that the presence of an equimolar

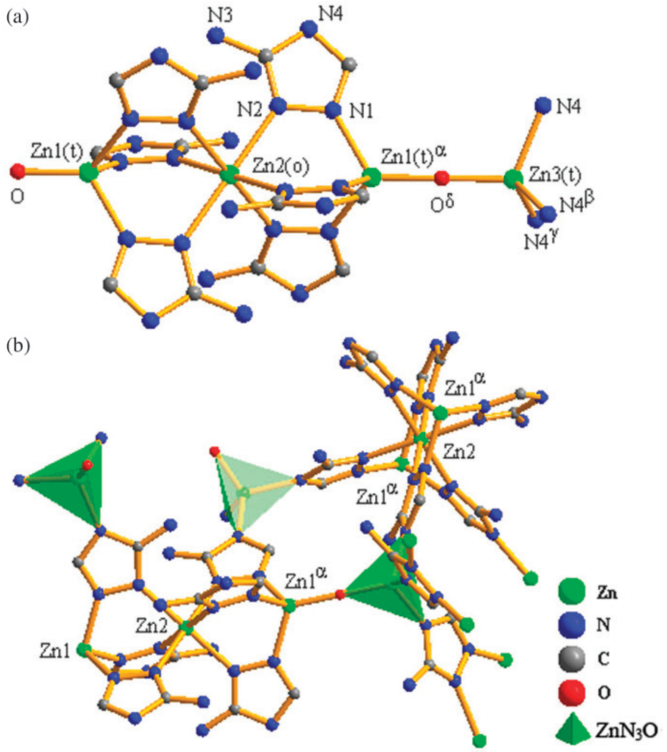

Figure 1. (a) Perspective view of coordination environments of the atrz anions in **1**·Zn. As a three-connected node, atrz links Zn1(t), Zn2(o) and Zn3(t) (t = tetrahedral coordination environment; o = octahedral coordination environment) atoms. (b) Perspective view of the linking relationship between the trinuclear linear $[Zn_3(atrz)_6]$ building blocks and the four-connected nodes of distorted tetrahedral $[ZnN_3O]$ in **1**·Zn (the disordered μ_2-O, represented by red spheres, are manually located on the axis along the Zn···Zn···Zn chain, for showing the green translucent tetrahedron. Hydrogen atoms are omitted for clarity; α: $x, -y+1/2, z-1/2$; β: $-y+1/2, -z+1, x+1/2$; γ: $z-1/2, -x+1/2, -y+1$; δ: $x, -y+1/2, z+1/2$).

amount of Zn^{2+} in the synthesis of the cobalt complex would induce formation of the isomorphous compound $\mathbf{1}\cdot Co(NO_3)_2(H_2O)_6$. In fact, the crystal structure of $\mathbf{1}\cdot Co(NO_3)_2(H_2O)_6$ for the ICP experiment showed homo-Co and no zinc(II).

3.2. *Structure description*

3.2.1. Two 3D isostructures of inclusion cages based on trinuclear linear Zn^{II}/Co^{II} building blocks. As shown in figure 1(a), the central Zn2 coordinates to six N2 donors of different μ_3-atrz anions, and each Zn1 coordinates to three N1 donors of different μ_3-atrz anions and one μ_2-O^{2-}, in the trinuclear linear Zn^{II} building blocks $[Zn_3(atrz)_6]$. The coordination mode of Zn3 is similar to that of Zn1, however, the former coordinates to three N4 donors of different μ_3-atrz anions and one μ_2-O^{2-}, as illustrated by the green translucent tetrahedron in figure 1(b). Zn1, Zn2, and Zn3 are all located on three-fold rotational axes; Zn2 is also located at the centrosymmetry site. As a three-connected node, atrz anion is bound to Zn1, Zn2 and Zn3 ions with its N1, N2 and N4 donors, correspondingly. None of the 3-amino substituents are coordinated. The Zn1···Zn2···Zn1 are arranged linearly and each of the terminal Zn1 ions are triply

Table 3. Summary of the structural characteristics of the compounds of related complexes.

Compound	Description of structure	Ref.
$[Zn_3(4Ettrz)_6(H_2O)_6](CF_3SO_3)_6$	Linear trinuclear with two triple *N*1,*N*2 triazole bridges	[44]
$[Zn_2(trz)_3(OH)]\cdot 3H_2O$	3-D, oct, $[ZnN_6]$ coordination geometry, $\{Zn(trz)_3\}_n^{n-}$ chains	[45]
$Zn_2(trz)_3Cl$	3-D, oct, $[ZnN_6]$ coordination geometry, $\{Zn(trz)_3\}_n^{n-}$ chains	[46]
$[Co_3^{II}(L^1)_8(NCS)_4](SCN)_2(H_2O)_9$	Linear trinuclear with two triple *N*1,*N*2 triazole bridges, 3.8828(9) Å ($Co^{II}\cdots Co^{II}$), L^1 = 4-*tert*-butyl-1,2,4-triazole	[47]
$[Co_3^{II}(HL^2)_6(NCS)_4F_2](H_2O)_2$	Co^{II} ions are bridged by two triazole units and one fluoride ion, $[CoN_4F_2]$ coordination geometry, 3.3726(3) Å ($Co^{II}\cdots Co^{II}$), HL^2 = 3,5-dimethyl-1,2,4-triazole	[48]
$[Co_3^{II}(L^3)_4(NCS)_4F_2(H_2O)_2](H_2O)_4$	Co^{II} ions are bridged by two triazole units and one fluoride ion, $[CoN_4F_2]$ coordination geometry, 3.4015(3) Å ($Co^{II}\cdots Co^{II}$), L^3 = 3,4,5-trimethyl-1,2,4-triazole	[49]
$[Co_2^{II}Co^{III}(HL^4)_2(L^4)_4(H_2O)_6]Cl_3(H_2O)_9$	Linear trinuclear with two triple *N*1,*N*2 triazole bridges, $[Co^{III}N_6]$ (Central), $[Co^{II}N_3O_3]$ (Terminal) coordination geometry, 3.653(3) Å ($Co^{II}\cdots Co^{II}$), HL^4 = 3,5-diamino-1,2,4-triazole	[50]
$Co_2(trz)_3Cl$	3-D, oct, $[CoN_6]$ coordination geometry, $\{Co(trz)_3\}_n^{n-}$ chains, 3.770(1) Å ($Co^{II}\cdots Co^{II}$)	[34]

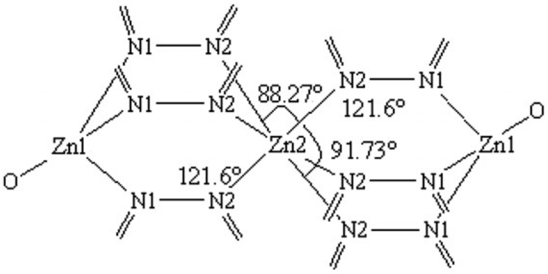

Scheme 1. Triple atrz *N*1,*N*2 bridging mode in trinuclear linear $[Zn_3(atrz)_6]$ building block.

bridged by three μ_3-atrz anions to the central Zn2 ion, consequently, trinuclear linear Zn^{II} building blocks, $[Zn_3(atrz)_6]$, are present (see figure 1a and 1b). The metal centers are separated by 3.5559(3) Å (3.5750(7) Å for that of Co subunit) from each other, and six amino groups of the bridging asymmetric triazoles point towards, but do not coordinate to the central Zn2 ion, in each $[Zn_3(atrz)_6]$ building block. The trinuclear linear Zn^{II}/Co^{II} subunit in which each M^{II} ion features an octahedral (or distorted octahedral) geometry are encountered in few discrete polynuclear complexes [44, 47–50], while the infinite $\{M(trz)_3\}_n^{n-}$ ($M = Zn^{II}/Co^{II}$) chains are observed in three polymers [34, 45, 46] (see table 3). By contrast with the common trinuclear linear chain, there are two distinct Zn^{II} coordination environments, Zn^{II} is distorted octahedral $[ZnN_6]$ (Zn = Zn2(o), *o* = octahedral coordination environment) sites and the two terminal zincs are distorted tetrahedral $[ZnN_3O]$ (Zn = Zn1(t), t = tetrahedral coordination environment) sites (see table 2 and scheme 1). Zn3 is a four-connected node of distorted tetrahedral $[ZnN_3O]$ (Zn = Zn3(t)) sites within **1**. The Zn^{II} centers of $[ZnN_3O]$ are coordinated to three μ_3-atrz of different trinuclear linear $[Zn_3(atrz)_6]$ building blocks *via* N4, and the centers are further connected by O^{2-} anions that act as

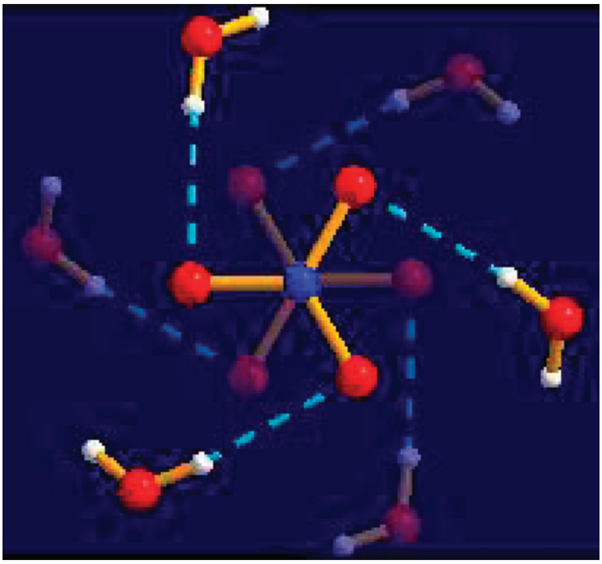

Figure 2. H-bonding network formed by the NO_3^- anions and water molecules in each pocket.

μ_2-bridging atoms to link the fourth building block through Zn1 ions (see figure 1b). The Zn1–O–Zn3, Zn–O and Zn1···Zn2 distances are 139.9°, 1.8806, 1.9200 and 3.5700 Å, respectively (140.7°, 1.8481, 1.9304 and 3.5750 Å for that of Co subunit) (see table 2). Thus, propagation of the structure in the crystal involves the trinuclear linear $[Zn_3(atrz)_6]$ building blocks and the distorted tetrahedral $[ZnN_3O]$ sites to generate a 3D architecture containing numerous cages in which 2n NO^{3-} and 6n H_2O are locked *via* noncoordinative interactions. There are hydrogen-bonding interactions between nitrates and solvent water molecules with an O_w–H···O distance of 3.03 Å ($\angle O_wHO = 173.7°$) [42], as shown in figure 2 by the translucent blue plane. Occupancy volumes for both the NO_3^- anions and water molecules are 926.3 $Å^3$ (**1** · Zn) and 952.7 $Å^3$ (**1** · Co), accounting for 27.2% and 28.0% of the total cell volumes, as calculated by PLATON [43]. Schematic presentation for the construction of the cage is portrayed in figure 3, and the perspective view of the 3D topology of **1** is shown in figure 4.

The isomorphous structure of **1** · Co is nearly an identical network with that of Zn (see figure S1 of the Supporting Information). It should be pointed out that the $Co^{II}···Co^{II}$ distance of trinuclear linear subunit is 3.5750(7) Å, considerably smaller than in other polymers [27, 34] (see table 3). Both tetrahedral and octahedral Zn^{II}/Co^{II} sites are present in the trinuclear linear Zn^{II}/Co^{II} systems, giving unprecedented 3D coordination polymers. There are few entities in which each M^{II} ion adopt octahedral coordination mode are observed in Zn^{II}/Co^{II} complexes of triazoles, up until now (see table 3).

3.3. *Thermal analyses*

Thermogravimetric profile (see figure S2 of the Supporting Information) of **1** · Zn showed 10.49% (ca 10.06%) weight loss between 139°C and 320°C, corresponding to

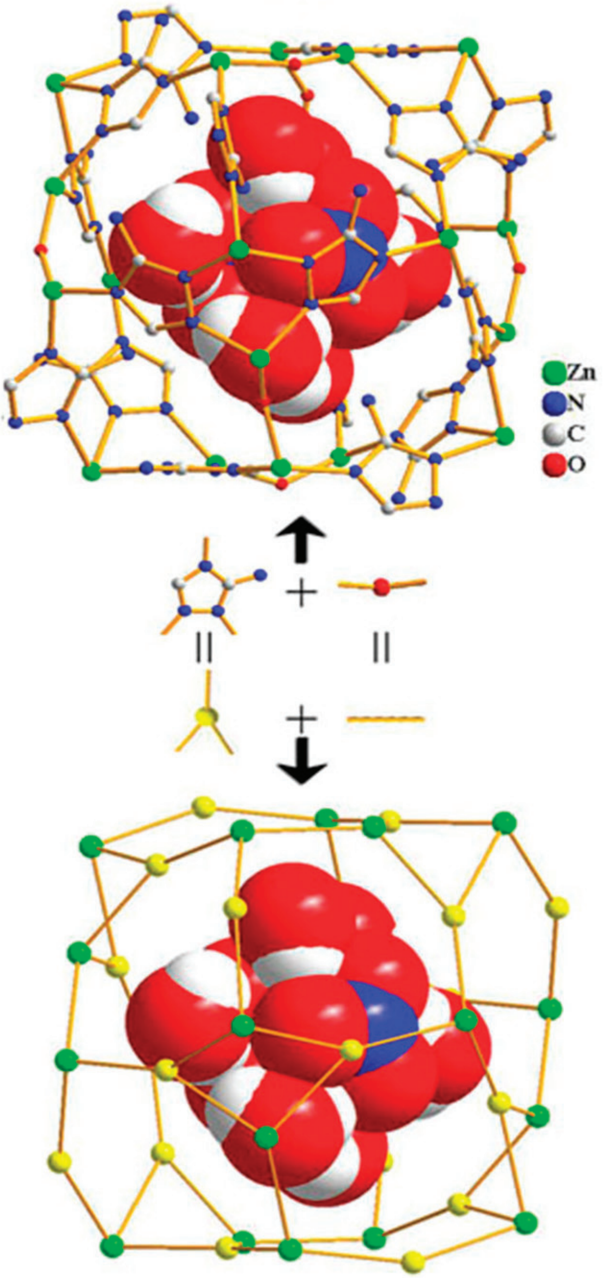

Figure 3. Schematic presentation for the construction of the cage in **1**·Zn. 2 NO_3^- and 6 H_2O shown by space-filling are locked in it. H atoms of the ligands are omitted for clarity in the top entity.

loss of H_2O located in the cages through two steps 139–240°C and 240–320°C. In contrast, there is only one step 4.56% (ca 5.19%) weight loss between 110°C and 260°C for **1** · Co, corresponding to loss of half the H_2O. The high temperature for loss of H_2O indicates difficult escape from the robust cages. After dehydration, two abrupt weight

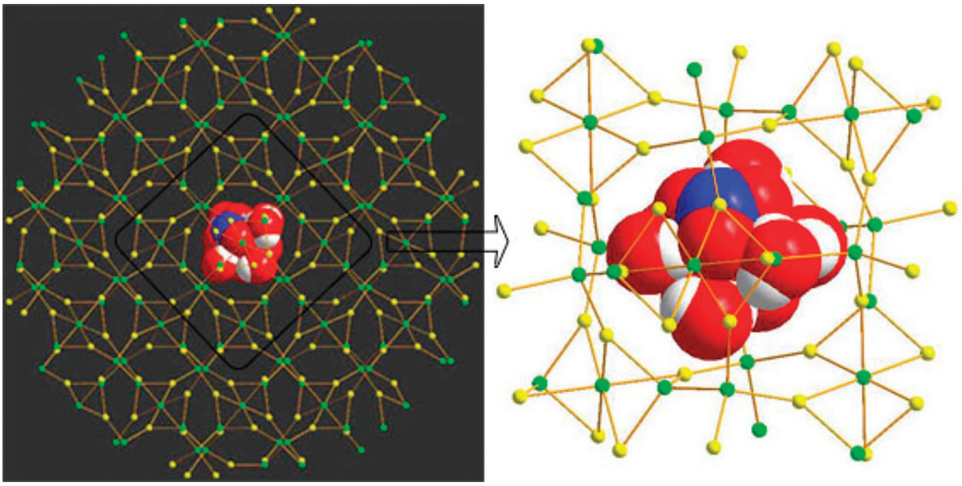

Figure 4. Perspective view of the 3D framework topology of **1**·Zn, along any one of the axes. $2NO_3^-$ and $6H_2O$ of one cage are shown by space filling.

losses of **1** · Co and **1** · Zn are indicated, corresponding to decomposition of framework and anions. Around 770°C for **1** · Zn and 620°C for **1** · Co, the residual ZnO and mixture of Co_2O_3 and CoO about 38.55% (ca 37.91%) and 40.80% are maintained.

Heating-cooling and dehydration-hydration experiments were carried out according to the TGA results. When **1** · Zn was heated to 240°C, the luster of the crystals disappeared and they changed from colorless to pale-yellow from loss of half of the water. In this first dehydration, the outside look of dehydrated solid was maintained. Further heating at 260°C led to second dehydration and distortion of the framework. The first dehydrated solid was obtained by heating **1** · Zn at 240°C for 30 min. The solid was immersed in water for 10 h and dried in air; there was a 5.6% weight loss observed, indicating that the first dehydration solid cannot rehydrate.

1 · Co was treated with similar methods, with similar results. The appearance of dehydrated solid was maintained until **1** · Co was heated to 256°C. The luster of crystals disappeared and the color changed to orchid ultimately.

Supplementary material

Crystallographic data have been deposited with the Cambridge Crystallographic Data Center, CCDC 619672 and 633361. Copies of this information can be obtained free of charge from The Director, CCDC, 12 Union Road, Cambridge, CB2 1EZ, UK (Fax: 44-1223-336-033; E-mail: deposit@ccdc.cam.ac.uk or www: http://www.ccdc.cam.ac.uk).

Acknowledgements

We gratefully acknowledge the financial support from the National Natural Science Foundation of China (Grant No. 20471047), NNSF of Shaanxi Province

(Grant Nos. FF05201 and FF05203), Shaanxi Physico-chemical Key Laboratory, Shaanxi Key Laboratory of Chemical Reaction Engineering and the Science and Technology Foundation of the National Defense Key Laboratory of Propellant and Explosive Combustion of China (Grant No. 51455010105QT3001).

References

[1] G.J. Halder, C.J. Kepert, B. Moubaraki, K.S. Murray, J.D. Cashion. *Science*, **298**, 1762 (2002).
[2] J.F. Eubank, R.D. Walsh, M. Eddaoudi. *Chem. Commun.*, 2095 (2005).
[3] O. Ohmori, M. Kawano, M. Fujita. *Angew. Chem.*, **117**, 1998 (2005); *Angew. Chem. Int. Ed.*, **44**, 1962 (2005).
[4] C.-D. Wu, W. Lin. *Angew. Chem.*, **117**, 1994 (2005); *Angew. Chem. Int. Ed.*, **44**, 1958 (2005).
[5] A.C. Sudhik, A.R. Millward, N.W. Ockwig, A.P. Côté, J. Kim, O.M. Yaghi. *J. Am. Chem. Soc.*, **127**, 711 (2005).
[6] O.R. Evans, W.B. Lin. *Acc. Chem. Res.*, **35**, 511 (2002).
[7] S.M. Kil, P.S. Myunghyun. *J. Am. Chem. Soc.*, **122**, 6834 (2000).
[8] B. Zhao, P. Cheng, X. Chen, C. Cheng, W. Shi, D.Z. Liao, S.P. Yan, Z.H. Jiang. *J. Am. Chem. Soc.*, **126**, 3012 (2004).
[9] A. Cingolani, S. Galli, N. Masciocchi, L. Pandolfo, C. Pettinari, A. Sironi. *J. Am. Chem. Soc.*, **127**, 6144 (2005).
[10] G. Ferey, C. Mellot-Draznieks, C. Serre, F. Millange. *Acc. Chem. Res.*, **38**, 217 (2005).
[11] S. Kitagawa, R. Kitaura, S.-I. Noro. *Angew. Chem. Int. Ed.*, **43**, 2334 (2004).
[12] S.R. Batten, R. Robson. *Angew. Chem. Int. Ed.*, **37**, 1461 (1998).
[13] G.S. Papaefstathiou, L.R. MacGillivray. *Coord. Chem. Rev.*, **246**, 169 (2003).
[14] X.L. Wang, C. Qin, E.B. Wang, Z.M. Su, L. Xu, S.R. Batten. *Chem. Commun.*, 4789 (2005).
[15] C. Livage, N. Guillou, J. Chaigneau, P. Rabu, M. Drillon, G. Frey. *Angew. Chem. Int. Ed.*, **44**, 6488 (2005).
[16] Y.H. Wen, J. Zhang, X.Q. Wang, Y.L. Feng, J.K. Cheng, Z.J. Li, Y.G. Yao. *New J. Chem.*, **29**, 995 (2005).
[17] S. Kitagawa, S. Noro. *Compr. Coord. Chem. II*, **7**, 231 (2004).
[18] C.N.R. Rao, S. Natarajan, R. Vaidhyanathan. *Angew. Chem.*, **116**, 1490 (2004); *Angew. Chem. Int. Ed.*, **43**, 1466 (2004).
[19] O.M. Yaghi, M. O'Keeffe, N.W. Ockwig, H.K. Chae, M. Eddaoudi, J. Kim. *Nature (London)*, **423**, 705 (2003).
[20] J.Y. Lu. *Coord. Chem. Rev.*, **246**, 327 (2003).
[21] S.L. James. *Chem. Soc. Rev.*, **32**, 276 (2003).
[22] J.G. Haasnoot. *Coord. Chem. Rev.*, **200–202**, 131 (2000).
[23] C.-Y. Su, A.M. Goforth, M.D. Smith, P.J. Pellechia, H.-C. zur Loye. *J. Am. Chem. Soc.*, **126**, 3576 (2004).
[24] M.H. Klingele, B. Moubaraki, J.D. Cashion, K.S. Murray, S. Brooker. *Chem. Commun.*, 987 (2005).
[25] O. Kahn, C.J. Martinez. *Science*, **279**, 44 (1998).
[26] M.H. Klingele, P.D.W. Boyd, B. Moubaraki, K.S. Murray, S. Brooker. *Eur. J. Inorg. Chem.*, 910 (2005).
[27] U. Beckman, S. Brooker. *Coord. Chem. Rev.*, **245**, 17 (2003).
[28] W. Li, H.-P. Jia, Z.-F. Ju, J. Zhang. *Crystal Growth & Design*, **6**, 2136 (2006).
[29] J.-K. Tang, H.-M. Wang, P. Cheng, X. Liu, D.-Z. Liao, Z.-H. Jiang, S.-P. Yan. *Polyhedron*, **20**, 675 (2001).
[30] Y. Garcia, P.J. van Koningsbruggen, H. Kooijman, A.L. Spek, J.G. Haasnoot, O. Kahn. *Eur. J. Inorg. Chem.*, 307 (2000).
[31] Y. Garcia, P.J. van Koningsbruggen, G. Bravic, D. Chasseau, O. Kahn. *Eur. J. Inorg. Chem.*, 356 (2003).
[32] Y. Garcia, J. Moscovici, A. Michalowicz, V. Ksenofontov, G. Levchenko, G. Bravic, D. Chasseau, P. Gutlich. *Chemistry-A European Journal*, **8**, 4992 (2002).
[33] K. Drabent, Z. Ciunik. *Chem. Commun.*, 1254 (2001).
[34] W. Ouellette, J.R. Galán-Mascarós, K.R. Dunbar, J. Zubieta. *Inorg. Chem.*, **45**, 1909 (2006).
[35] G.M. Sheldrick. *SADABS. Software for Empirical Absorption Corrections*, University of Göttingen, Gemany (2000).
[36] G.M. Sheldrick. *SHELXS-97, Program for Solution of Crystal Structures*, University of Göttingen, Germany (1990).
[37] G.M. Sheldrick. *SHELXL-97, Program for Refinement of Crystal Structures*, University of Göttingen, Germany (1997).

[38] C.-Y. Su, A.M. Goforth, M.D. Smith, P.J. Pellechia, H.-C. zur Loye. *J. Am. Chem. Soc.*, **126**, 3576 (2004).

[39] Deprotonation of the 1,2,4-triazole ligand (p*K*a = 2.25[25]) is found to be a common feature of its hydrothermal chemistry in the presence of metals, and a shift in p*K*a is found to occur under hydrothermal conditions [40]. Therefore, it is understandable that Hatz (p*K*a = 4.04[27]) takes the deprotonated form to participate in metal ion coordination under slightly acidic reaction conditions. The pH of a typical reaction mixture before reaction is about 4. The use of Hatc may give a more acidic reaction mixture, but because it undergoes decarboxylation to become Hatz, deprotonation is still expected.

[40] D.J. Chesnut, A. Kusnetzow, R. Birge, J. Zubieta. *Inorg. Chem.*, **38**, 5484 (1999).

[41] D.W. Wiley, O.W. Webster, E.P. Blanchard. *J. Org. Chem.*, **41**, 1889 (1976).

[42] G.A. Jeffery. *An Introduction to Hydrogen Bonding*, Oxford University Press, New York (1997).

[43] A.L. Spek. *Acta Crystallogr., Sect. A*, **46**, C-34 (1998).

[44] A.L. Spek, G. Vos. *Acta Crystallogr., Sect. C*, **39**, 990 (1983).

[45] W. Ouellette, B.S. Hudson, J. Zubieta. *Inorg. Chem.*, **46**, 4887 (2007).

[46] Q.-G. Zhai, X.-Y. Wu, S.-M. Chen, C.-Z. Lu, W.-B. Yang. *Crystal Growth & Design*, **6**, 2126 (2006).

[47] L.R. Groeneveld, R.A. Le Fèbre, R.A.G. de Graaff, J.G. Haasnoot, G. Vos, J. Reedijk. *Inorg. Chim. Acta*, **102**, 69 (1985).

[48] F.J. Rietmeijer, G.A. van Albada, R.A.G. de Graaff, J.G. Haasnoot, J. Reedijk. *Inorg. Chem.*, **24**, 3597 (1985).

[49] F.J. Rietmeijer, J.G. Haasnoot, A.J. den Hartog, J. Reedijk. *Inorg. Chim. Acta*, **113**, 147 (1986).

[50] L. Antolini, A.C. Fabretti, D. Gatteschi, A. Giusti, R. Sessoli. *Inorg. Chem.*, **30**, 4858 (1991).